


Concurrent efficient entanglement routing for quantum wireless networksWeicong Huang^{1,*}, Dong Jiang² and Lijun Chen^{1,†}¹*State Key Laboratory for Novel Software Technology, Nanjing University, Nanjing 210046, China*²*School of Internet, Anhui University, Hefei 230039, China* (Received 4 October 2021; revised 12 February 2022; accepted 13 April 2022; published 27 April 2022)

Due to the unconditional security of quantum communication and flexible and economical implementation of wireless communication, quantum wireless networks (QWNs) have attracted wide attention. Different from fiber-based or satellite-based quantum communication, quantum wireless networks have the characteristics of high dynamics, limited node energy, and quantum resource competition. We have found that the existing quantum wireless network routing protocols suffer from path collision, high energy consumption, and low utilization of quantum resources. In this paper, a more practical and efficient entanglement routing protocol, which can find contention-free paths for concurrent source destination pairs, is proposed. Simulation results show that the proposed protocol can not only greatly improve the throughput and success rate of the network, but also significantly prolong the network lifetime. The research developed by this work may stimulate more investigations of entanglement routing problems in QWNs.

DOI: [10.1103/PhysRevA.105.042619](https://doi.org/10.1103/PhysRevA.105.042619)**I. INTRODUCTION**

The security of classical communication cryptosystems is based on the computational complexity of certain functions such as factorization of large numbers. With the tremendous progress in superconducting qubits [1], trapped ions [2], nitrogen-vacancy centers in diamond [3], integrated photonics [4], etc., quantum computation poses a great threat to classical communication. As opposed to classical communication, quantum communication embraces the unconditional security guaranteed by the laws of quantum mechanics [5,6]. Since point-to-point quantum key distribution (QKD) communication is limited by distance, large-scale quantum networks have been proposed and researched [7–11]. Many experimental studies have successfully implemented quantum networks for long-distance communication in the field, such as the DARPA quantum network [10], the SECOQC Vienna QKD network [12], the Tokyo QKD network [13], and China's satellite quantum network [14]. These quantum networks are all based on optical fiber or satellite communication. Fiber-based quantum networks [13,15–17] can be quickly deployed in existing classical communication networks, whereas it is limited by the fixed distribution of infrastructures. Satellite-based free-space quantum communication [14] exploits lower loss in the empty space than fiber-based networks to establish longer quantum links. However, the quantum links can only be established for certain ground locations within a limited time window.

To exceed the limits of existing quantum communication methods, Liu *et al.* [18] propose drone-based quantum wireless networks, which can offer secure coverage in real time without being affected by fixed infrastructures and regions.

Compared with fiber-based and satellite-based quantum networks, quantum wireless networks (QWNs) are more flexible and economical, which can be applied in many different fields including real-time surveillance [19], rescue and recovery operations [20], reconnaissance operations [21], wind estimation [22], and so on [23–27]. Although QWNs have many advantages, the mobility and finite energy of nodes make the routing and data transmission more complicated than other types of quantum networks. We would like to realize efficient end-to-end entanglement routing protocol in QWNs.

Currently, the existing quantum wireless network protocols can be divided into three categories. The first category [28] is the quantum relay routing scheme, which relies on trusted repeaters and the actual qubit information can be obtained by intermediate forwarding nodes. It is similar to the store-and-forward process in classical networks. Since the quantum network with trusted nodes does not provide end-to-end security, the trusted nodes need extra physical security mechanisms to protect. The second category [29–35] focuses on designing the quantum network architecture and teleportation schemes based on different quantum states, in which the routing mechanism is not discussed and the paths are assumed to have been selected appropriately. The third category [36,37] utilizes quantum repeaters to establish long-distance entanglement through entanglement swapping and transmit information from one end to the other. However, such protocols ignore certain realities in QWNs, such as concurrent requests for resources, arbitrary topology, the dynamics and exclusivity of quantum links, and the limited energy of nodes. Due to path conflicts and resource contention in the concurrent communication of nodes, the third category is treated as quantum competitive path selection (QCPS) routing protocols.

In this paper, we first propose a concurrent and efficient entanglement routing protocol for QWN, which can solve the problems of path collision, high energy consumption, and low

*huangwc@smail.nju.edu.cn

†chenlj@nju.edu.cn

utilization of quantum resource. A different model, metrics, and algorithms are presented in the protocol. To verify the performance of the protocol, a custom-built simulator [38] which supports topology generation and statistics is provided. The performance is evaluated in various parameters through simulations and the results demonstrate that the proposed protocol has a higher throughput and success rate than QCPS routing protocols.

The rest of the paper is organized as follows. Section II discusses the challenges involved in QWN routing. Section III introduces the basic concepts of quantum routing protocol. Section IV provides the proposed communication protocol. Section V gives the performance evaluations of the proposed protocol and the existing protocol. The conclusion and prospects for future work are presented in Sec. VI.

II. CHALLENGES INVOLVED IN ROUTING

Quantum wireless networks are a category of decentralized infrastructureless networks. They have the advantages of convenience and security. Compared with other types of networks, QWNs still face many challenges in routing. In the following we list and analyze them.

QWNs versus routing in classical packet-switching wireless networks. Proactive routing protocols [39] and reactive routing protocols [40] are the two main types of routing protocols for classical wireless networks. One sends a message to the other and the message is split into small packets and spreads independently in the network. When the network is congested, the packets can be buffered on any node and retransmitted until the receiver acknowledges it. In QWNs, (i) quantum states cannot be copied due to the quantum no-cloning theorem and (ii) each source-destination (SD) pair must occupy a quantum channel exclusively. Hence the optimal paths computed by classic routing are not always available without considering resource competition. (iii) Since entanglements on the quantum links are delicate and decay quickly, all hops of the path should have at least one successful quantum links in one time slot to establish an end-to-end entangled link.

QWNs versus routing in fiber-based and satellite-based quantum networks. For fiber-based or satellite-based quantum networks, such as those in Refs. [41–44], the calculation of feasible paths is based on known global network topology information. For QWNs, intermittent movement of nodes leads to unpredictable position changes in the network topology. Since the quantum states are delicate and entanglements on the quantum links decay quickly, there is no time to broadcast the global network topology information.

QWNs versus routing in circuit-switching networks. Although both the circuit-switching network [45–47] and QWNs need to predetermine the end-to-end path and reserve resources on the path, they still have differences. (i) The topology in QWNs is dynamic, while the topology in circuit-switched networks is stable. Therefore, the routing algorithms in the two types of networks are different. (ii) In QWNs, two adjacent nodes need to establish at least one quantum entangled link and all nodes on the channel need to perform entanglement swapping in one time slot. Since the quantum entanglements may fail randomly with a certain probability,

we propose a path recovery phase to increase the success probability of establishing end-to-end quantum entanglement.

QWNs versus routing in existing quantum wireless networks. The QCPS protocol differs from the proposed protocol in the following ways. (i) The conflict and competition for quantum resources are not considered in routing path selection in QCPS. That is, regardless of whether the selected path is already occupied by other requests, the algorithm will directly select a path with the best metrics. (ii) Entangled photon pairs are first distributed among all adjacent nodes in QCPS, followed by the routing phase. This scheme will lead to low utilization of quantum resources and high energy consumption when the number of requests is small. (iii) Route request and route finding is implemented by flooding in QCPS. Flooding takes up a substantial amount of network bandwidth and consumes more energy, which is at a premium in wireless networks. Overall, QCPS routing protocols cannot adequately solve the problems in QWNs.

III. PRELIMINARIES

In the following we introduce the basic concepts in routing protocols including entanglement, quantum teleportation, and entanglement swapping. More details of the quantum mechanism can be found in Ref. [48].

Entanglement. Entanglement, which Einstein referred to as “spooky action at a distance,” is the condition of a quantum state in which the states of subsystems are not independent: Operations on one part of the system can affect the state of other parts, regardless of physical distance. The first entanglement-based quantum key distribution protocol was proposed by Ekert [8]. Entanglement comes in many forms and can involve more than two parties, but in this paper we focus on the two-party Bell states, which are usually written

$$|\psi^\pm\rangle = \frac{1}{\sqrt{2}}(|01\rangle \pm |10\rangle), \quad |\phi^\pm\rangle = \frac{1}{\sqrt{2}}(|00\rangle \pm |11\rangle). \quad (1)$$

Teleportation and entanglement swapping. Due to Heisenberg’s uncertainty principle and quantum no-cloning theorem [6], an arbitrary unknown quantum state cannot be measured precisely or replicated perfectly. However, the unknown quantum states can be teleported reliably from one system to another over arbitrary distances. Entanglement swapping [9] can be understood as a special case of the teleportation protocol, where the teleported quantum system is itself entangled. Two short-distance entangled pairs can be spliced into one longer-distance entangled pair by entanglement swapping.

As seen in Fig. 1, Alice and Charlie are far away from each other and can generate entanglement with Bob’s assistance. Two entangled pairs of photons a - b_1 and b_2 - c are produced by Alice and Charlie, respectively. One photon from each pair is sent to Bob, who subjects them to a Bell-state measurement (BSM), projecting them randomly into one of four possible entangled states. This procedure projects photons a and c into a corresponding entangled state.

The teleportation protocol is sketched in Fig. 2. At entanglement swapping, Alice and Charlie each have one qubit of an entangled pair (qubits a and c) in the joint state $|\Psi^+\rangle_{ac} = \frac{1}{\sqrt{2}}(|01\rangle + |10\rangle)$. Alice is in possession of the state (qubit d) to be teleported, which is most generally given by $|\varphi\rangle_d =$

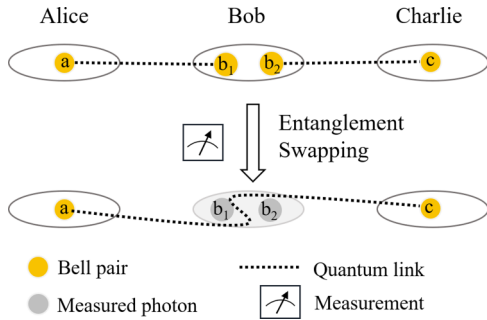


FIG. 1. Entanglement swapping version of quantum teleportation. The yellow circles (dotted lines) represent entangled qubits (quantum links).

$\alpha|0\rangle + \beta|1\rangle$. The combined state of all three qubits can be expressed as

$$\begin{aligned}
 |\varphi\rangle_d \otimes |\Psi^+\rangle_{ac} = & \frac{1}{2}(|\Phi^+\rangle_{da} \otimes (\alpha|1\rangle + \beta|0\rangle)_c \\
 & + |\Phi^-\rangle_{da} \otimes (\alpha|1\rangle - \beta|0\rangle)_c \\
 & + |\Psi^+\rangle_{da} \otimes (\alpha|0\rangle + \beta|1\rangle)_c \\
 & + |\Psi^-\rangle_{da} \otimes (\alpha|0\rangle - \beta|1\rangle)_c. \quad (2)
 \end{aligned}$$

To teleport the quantum state to Charlie, Alice performs a joint measurement on her qubits (qubits d and a) in the Bell basis. Then Alice sends the outcome via a classical communication channel to Charlie, who can then recover the original state by applying the corresponding local transformations.

IV. ENTANGLEMENT ROUTING PROTOCOL

In this section we propose the quantum contention-free path selection and one-hop-based path recovery (QCFPSR) routing protocol, which takes into account the dynamics of network topology, vulnerability of quantum links, node energy depletion, and concurrent requests of SD pairs. Compared with QCPS, our protocol is more in line with existing physical experiments and theoretical studies [9,11,15,18,49]. In the following we first introduce the network components. Then the routing metrics and protocol procedures are presented in detail.

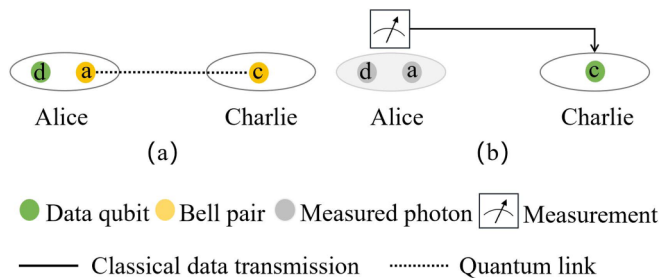


FIG. 2. Long-distance data qubit transmission based on teleportation. (a) Alice and Charlie share long-distance entanglement after entanglement swapping in Fig. 1. (b) Alice performs a BSM to teleport qubit d to Charlie.

A. Network components

We represent the quantum network with the graph $G = \langle V, C, L \rangle$, where V is the set of mobile quantum nodes, C is the set of lossy free-space channels between two nodes, and L is the set of quantum links on these channels.

Quantum nodes. Each quantum node is a processor equipped with quantum memory and necessary hardware to perform entanglement distribution and quantum teleportation. All nodes are connected to other quantum nodes through quantum channels and a classic network to form a quantum network, which can exchange classic and quantum information freely. Due to the beam diffraction and energy loss when photons propagate in free space [52], it is difficult to directly establish entanglement between two remote nodes. Therefore, each node will also be used as a quantum repeater [50,51] to achieve long-distance entanglement sharing via entanglement swapping.

Quantum channels. The source and the destination nodes establish quantum channels in free space for secure communication. For each quantum channel C_{ij} , the nodes i are capable of generating W_{ij} quantum links in parallel with its neighbor node j in a fixed time T . The channel width W_{ij} is defined as

$$W_{ij} = \frac{Tc}{L_{ij}}, \quad (3)$$

where L_{ij} is the length of a quantum link between adjacent nodes and c is the speed of light in the communication channel. A path is identified by the sequence of the nodes along the path and the path width W means that each channel on the path has at least W parallel quantum links.

Quantum links. The establishment of entanglement between any two nodes indicates the success of the quantum link. The link success rate P_{ij} of sharing a pair of entangled photons between two nodes i and j of length L_{ij} is $e^{-\gamma L_{ij}}$, where γ is the attenuation coefficient that depends on the absorption and scattering of molecules and aerosol particles present in the air [52]. If the link distance is over the Rayleigh length limit, the beam aperture will be divergent and become larger than the receiver telescope, which inevitably introduces loss to the system. Therefore, the communication range of our neighboring nodes is not greater than the maximum communication radius R . Since the quantum link is dynamic, the establishment of quantum entanglement may fail with a certain probability. The actual number of quantum links on a channel is less than or equal to the channel width W_{ij} . The quantum channel success rate $P_{C_{ij}}$ at which at least one entangled link is established successfully across the channel C_{ij} is defined as

$$P_{C_{ij}} = 1 - (1 - P_{ij})^{W_{ij}}. \quad (4)$$

B. Routing metrics

Our routing metrics is based on the following three factors to design the protocol and make routing decisions. Below we will discuss these aspects in detail.

1. Residual energy

In wireless networks, mobile nodes such as drones are powered by batteries and have a limited energy supply. Over

time, energy supplies will be depleted and nodes will drop out from the network. In a large network, almost all source nodes rely on quantum repeaters to generate long-distance entanglement since they cannot communicate directly with destinations. Therefore, designing an efficient routing protocol to control and decrease consumed power can prolong the network lifetime. Assuming that the minimum energy required by a node to complete classical and quantum communications in one time slot is E_{\min} , the node will enter the sleep state if the node energy is less than E_{\min} . The energy of mobile nodes is depleted in the following ways.

(a) *Energy consumption in classic communication.* The wireless communication module has four states: send, receive, idle, and sleep. The sending and receiving processes account for about two-thirds of its total energy consumption. The energy consumed in transmitting depends on the length of the message and the transmission distance, and the energy consumed in receiving depends on the length of the message [53].

(b) *Energy consumption in quantum communication.* The energy consumption of the quantum communication system mainly includes the preparation of quantum states, BSM, storage of entangled photon states, gated mode operation, and acquiring, pointing, and tracking systems.

2. Width of quantum channel

The establishment of end-to-end entanglement requires numerous attempts at entanglement distribution on each quantum channel or entanglement swapping along the path. The probability of successful entanglement distribution or entanglement swapping performed by repeaters increases with path width W . Since the entangled link is highly dynamic and delicate, it may fail randomly in one time slot. Therefore, the wider paths are more reliable and preferred.

3. Node distance

The source node will select a suitable neighbor node as a quantum repeater when the distance between the source and the destination nodes exceeds the communication radius. For an intermediate node, it is more inclined to choose the neighbor node closer to the destination as the next hop. Routing with fewer hops consumes less energy than more hops for any request, which can also reduce the end-to-end delay and increase the success rate after swapping. Below we define the Euclidean distance between nodes A and D as

$$\text{Dist}(A; D) = \sqrt{(x_1 - x_2)^2 + (y_1 - y_2)^2}. \quad (5)$$

The node location is defined by an $(x; y)$ coordinate pair, where $(x_1; y_1)$ are the coordinates of intermediate node A and $(x_2; y_2)$ are the coordinates of destination node D .

Further, considering the entanglement swapping success rate q and average link success rate P_L , along a path comprising h hops and of width W , the number N_{el} of shared entangled links per time slot between the end points of the path is defined as

$$N_{el} = W q^{h-1} \prod_{j=1}^h [1 - (1 - P_L)^{W_{ij}}], \quad (6)$$

where $i = j - 1$ and P_L is a simplification of P_{ij} . According to Eq. (6), we can draw the following conclusions. (i) A path with fewer hops and greater widths has a higher number of successful entangled links. (ii) In practice, paths with long-distance links have fewer hops but are also narrower; paths with multiple shorter-distance links have more hops but are also wider.

Since the energy supply is limited in QWNs, routing with fewer hops consumes less energy than more hops for any request, which can also reduce the end-to-end delay and increase the success rate after entanglement swapping. Therefore, node distance is the primary consideration in routing metrics. Since the probability of successful entanglement distribution or entanglement swapping performed by repeaters increases with path width W , channel width is used as a metric when multiple node distances are the same in routing.

C. Routing protocol

In the following we present the QCFPSR routing protocol, which is designed to find (i) the optimal paths for multiple concurrent requests which are contention-free on quantum channels and (ii) the recovery paths for the failed entangled links. We assume that time is slotted and the time synchronization among all nodes can be achieved by existing current synchronization protocols [54] via the Internet. As shown in Fig. 3, each time slot contains four phases and is set to an appropriate duration such that the established entangled links will not be decoherent within one time slot [21].

Phase 1. First is the major path discovery phase. Source nodes concurrently request to establish long-distance quantum entanglements with the destination nodes via the Internet [55]. This process includes the construction of a candidate neighbor table (CNT), node forwarding, and path optimization.

Construction of a CNT. For our edge-disjoint routing protocol, each node in the quantum network maintains a candidate list. In the list, each CNT (as shown in Fig. 4) contains neighbor ID, neighbor position, quantum channel width, and quantum channel state. Each node has a unique ID to identify itself. The location information of each node can be obtained by using GPS [56] or a distributed localization scheme based on the received signal power [57–59], etc. Each node periodically transmits beacons to the broadcast the information about its own ID and position. Once a beacon is not received from a neighbor for longer than a timeout interval, the node supposes that the neighbor has been out of range or failed and deletes the neighbor from its CNT. Similarly, the locations of the destination nodes could be obtained via an information relay system. The quantum channel width can be calculated according to Eq. (3). Since the quantum resources are reserved exclusively, the quantum channel state is set to a Boolean value, which is 0 or 1 when the quantum channel is idle or occupied, respectively. The initial value of the quantum channel state is 0.

Greedy forwarding. When the source node wants to communicate with the destination node, a route request (RREQ) packet is created and presented in the formatting as shown in Fig. 5(a). The source ID, destination ID, and request ID can jointly identify a specific route discovery. The last hop ID field records the neighbor ID from which the RREQ is received, the

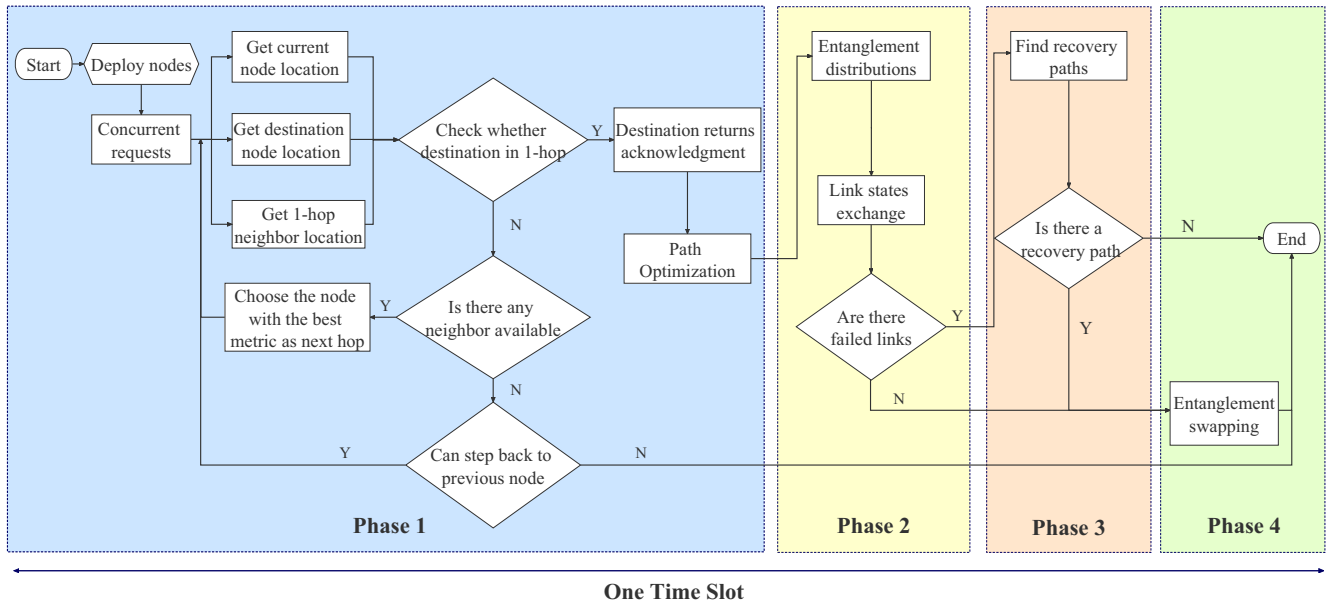


FIG. 3. Flowchart of the quantum wireless network routing protocol.

next hop ID records the neighbor that is expected to receive or forward the RREQ, and the hop count is the number of route forwarding. The value of the hop count is initialized to 0 and is incremented by 1 for each forwarding. The source node calculates the distance between all neighbor nodes with idle quantum channel states in the CNT and the destination node and select the neighbor node closest to the destination node as the next hop. If multiple nodes have the same distance to the destination node, the source node will select the node with the maximum channel width W_{ij} as the next hop and then update the information in the CNT and RREQ, where the quantum channel state of the next hop node in the CNT is set to 1, and the node ID, neighbor ID, and updated hop count are recorded as the last hop ID, next hop ID, and hop count in the RREQ, respectively.

The source node broadcasts the RREQ packet. When another intermediate node receives a RREQ packet from its neighbor, it first checks the corresponding next hop ID and destination ID. If the intermediate node is the destination node, it first sets the quantum channel state of the previous hop node in the CNT to 1, then stops forwarding the RREQ, and starts the path optimization process. For the intermediate node expected to forward the RREQ, it checks whether all neighbor nodes are unavailable in the CNT or it has forwarded the RREQ before. If not, the intermediate node first sets the quantum channel state of the previous hop node in the CNT to 1, then updates the RREQ packet and routing table [as shown

Candidate List	Neighbor ID
	Neighbor Position
	Quantum Channel Width
	Quantum Channel State

FIG. 4. Structure of the candidate neighbor table entry.

in Fig. 5(b)], and continues to forward RREQ. Otherwise, the intermediate node starts the step back process.

Step back. During the exploration of the routing path, the intermediate node will not further forward the received RREQ when there are no available neighbor nodes in the CNT or the node has already forwarded the RREQ. In this case, the intermediate node will step back to its previous hop node. After the previous hop node receives the message, it will first set the corresponding quantum channel state in the CNT to 0 and then attempt to find another available neighbor node as the next hop node. The procedure will be repeatedly executed until the RREQ is sent to the destination node or the hop count reaches h_{max} , the maximum number of hops.

Path optimization. Once the path between the source and destination nodes is established, a successful acknowledgment is sent back from the destination to the source node. During the reverse acknowledgment process, the number of redundant hops in the path can be reduced by optimization. First, the destination node broadcasts a request ID to all its neighbors. The neighboring node with the same request ID will send a reply message with the hop count. Then the destination node sends an acknowledgment to the neighbor with the smallest number

Source ID
Destination ID
Request ID
Last Hop ID
Next Hop ID
Destination Position
Hop Count

(a)

Source ID
Destination ID
Hop Count
Last Hop ID
Next Hop ID
Request ID

(b)

FIG. 5. (a) Format of the RREQ packet. (b) Structure of the routing table entry.

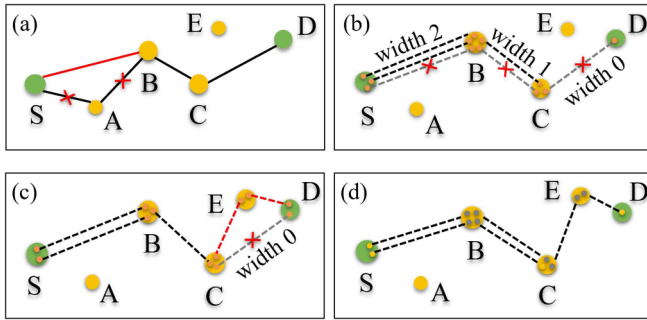


FIG. 6. Flowchart of quantum wireless network routing protocol. (a) Node forwarding and path optimization. (b) Entanglement distribution and link states exchange. (c) Path recovery. (d) Entanglement swapping.

of hops and sends a release command to all intermediate nodes that are not used for transmission. The node receiving the release command first finds the last hop ID and the next hop ID in the routing table according to the request ID and then sets the quantum channel states of the corresponding nodes to 0 in the CNT and deletes the related routing table entries. The node receiving the acknowledgment first checks the next hop ID in the routing table according to the request ID and sets the quantum channel state of the next hop node to 0 in the CNT. Then the node modifies the next hop ID in the routing table and continues the path optimization process. The major path is established [as shown in Fig. 6(a)] when the source node receives a successful acknowledgment. Otherwise, the source node will not continue and waits to initiate the request again in the next time slot. In phase 2, nodes on the path start to establish entangled pairs with neighbors.

Phase 2. This is the entanglement distribution and link state exchange phase. As shown in Fig. 6(b), nodes on each channel of the path make W_{ij} attempts to generate and establish quantum entanglements with its neighbor nodes. As long as an entangled link is successfully established, we consider the entanglement distribution on that channel to be successful. Since the entangled links are highly dynamic and decay quickly and classical networks have delays, it is impractical for a node to know the global quantum link states within such a short time. Thus, each node only exchanges the quantum link states with its one-hop neighbors via the classical network.

Phase 3. This is the recovery path discovery phase. If entanglement distributions on all quantum channels of the path are successful, the node will enter phase 4 and perform entanglement swapping to establish long-distance end-to-end entanglement. In practice, the quantum link is delicate and entanglement distributions have a high probability of failure. Therefore, after finding the major paths, the remaining quantum resources will be utilized to construct recovery paths. For each quantum channel that fails to establish entangled links, phases 1 and 2 are repeated to find and establish the recovery paths until no more paths are found or time is up. If there are no available recovery paths, the failed nodes inform other nodes on the path with a termination message. As shown in Fig. 6(c), a recovery path from node C to node D through node E is found and the entangled links are successfully established.

Phase 4. This is the entanglement swapping phase. All nodes on the path make swapping decisions consistently and perform entanglement swapping locally to establish long-distance entanglement. If entanglement swapping fails, the node will inform the source node with an error message. Otherwise, entanglement between source node S and destination node D is established. As shown in Fig. 6(d), nodes B, C, and E perform BSM on the corresponding qubits in their hands, respectively, and two long-distance entangled links between S and D and between S and C are established.

After the above four phases, the source node will teleport the qubits to the destination node successfully and the secret information can be obtained securely. The unused quantum entangled links will be discarded and the information in the CNT and routing table is reset to empty. Then the next round of communication is started.

V. SIMULATION AND PERFORMANCE EVALUATION

In this section we build a custom simulator [38] to evaluate the performance of the QCPS, QCFPSR, and QCFPSR without a recovery path discovery phase (QCFPSR-WR) protocols. We use the existing routing protocol [36] as the representative of the QCPS routing protocols, which has the same routing metrics as our proposed protocol. Since additional overhead of the path recovery phase compared to the QCPS protocol would necessitate longer time, we also simulate the QCFPSR-WR protocol to prove the superiority of our protocol performance. In the following sections we first briefly introduce the QCPS protocol, then the simulation environment and performance metrics are given, and finally we run simulations to compare the results in a number of parameter settings and investigate the impact of various parameters on the performance.

A. QCPS routing protocol

The QCPS routing protocol proposes a multihop communication model with quantum teleportation and a quantum routing algorithm. The number of hops was selected as a route metric, which is the same as our proposed protocol. In the following we introduce the four phases of the protocol briefly; the details can be found in Ref. [36].

(i) *Entanglement distribution.* All nodes in the network first attempt to generate and establish entangled links with their neighbor nodes.

(ii) *Quantum route request.* When the source node wants to communicate with the destination node, it first checks whether there is an available route to the destination node. If no routes are available, the source node broadcasts the quantum route request (QRR) packet, which contains the number of hops through the wireless channel to create a route.

(iii) *Quantum route finding.* When the destination node receives the QRR, the route selection and route reply phases begin. The destination node selects the path with the least number of hops and the quantum and classical routes existing simultaneously as the route. If there is more than one route satisfying these conditions, the destination node chooses the one whose QRR is first received by the destination. Then the destination node unicasts a reply message to the source node

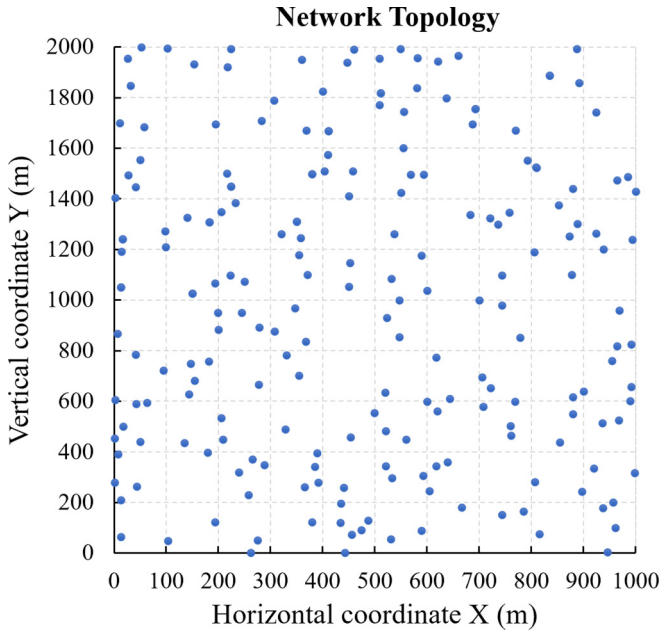


FIG. 7. Network topology (200 nodes) diagram of experimental simulation. The blue dots represent the quantum nodes and the label represents the node ID.

by the reverse route. The route is successfully established when the source node receives the reply message.

(iv) *Entanglement swapping.* All nodes on the path perform entanglement swapping to establish long-distance quantum entanglement. If the end-to-end quantum entanglement is established successfully, the quantum state can be directly teleported from the source node to the destination node. So far, the quantum communication process has been successfully completed.

B. Simulation environment

The custom-built simulator [38] supports network topology generation and statistics, which do not assume any specific network topology and randomly generate quantum networks

for simulations. We deploy N quantum nodes randomly on a $2000 \times 1000 \text{ m}^2$ site. All the nodes in the network are considered trustworthy and willing to participate. The QCPS, QCFPSR, and QCFPSR-WR protocols share the same network node distribution and node configuration. A sample of node deployment is shown in Fig. 7 and the simulation parameters are summarized in Table I.

To control variables, we show the results under the reference setting $N = 200$, $M = 8$, $N_{TS} = 1000$, $P_{ES} = 0.9$, and $P_L = 0.8$ unless explicitly changed to observe the data trend. For each setting of N , M , N_{TS} , P_{ES} , and P_L , we simulate N_{TS} consecutive time slots in the networks. In each time slot, SD pairs are randomly selected. The experimental simulation runs on a 64-bit Windows 10 system with 16 GB memory and i7-10710U processor.

C. Performance metrics

We primarily consider the following four performance metrics.

(i) *Throughput.* The purpose of the routing protocol is to satisfy all concurrent communication requests and maximize the number of entangled states between each SD pair. The throughput quantifies the number of entangled qubit per one time slot of all SD pairs in the entire network.

(ii) *Success rate.* The success rate represents the probability of one SD pair successfully establishing a quantum channel in one time slot, as shown by

$$\text{success rate} = \frac{\text{No. of successful SD pairs}}{\text{No. of concurrent SD pairs}}. \tag{7}$$

(iii) *Average energy.* The node average energy quantifies the average residual energy of all nodes throughout the simulation time, as shown by

$$\text{average energy} = \frac{\text{total residual energy}}{\text{No. of nodes}}. \tag{8}$$

(iv) *Number of nodes.* The number of active nodes indicates the network lifetime over time. The node will enter the sleep mode when the residual energy is below E_{\min} .

TABLE I. Initial parameters for the node configuration.

Parameter definition	Symbol	Default	Value
Node communication radius	R		200 m
Node distribution range			$1000 \times 2000 \text{ m}^2$
Time of entanglement distribution	T		$1.5 \mu\text{s}$
Number of concurrent SD pairs	M	8	2, 4, 6, 8, 10
Total number of nodes	N	200	100, 150, 200, 250, 300
Number of time slots	N_{TS}	1000	1000, 2000, 3000, 4000, 5000
Average link success rate	P_L	0.8	0.5, 0.6, 0.7, 0.8, 0.9
Node initial energy	E		60 J
Node minimum energy	E_{\min}		2 J
Message transmission energy	E_{TX}		$50 \mu\text{J}$
Message receiving energy	E_{RX}		$10 \mu\text{J}$
Entanglement swapping energy	E_{ES}		1 mJ
Entanglement distribution energy	E_{ED}		1 mJ
Entanglement swapping success rate	P_{ES}	0.9	0.6, 0.7, 0.8, 0.9, 1

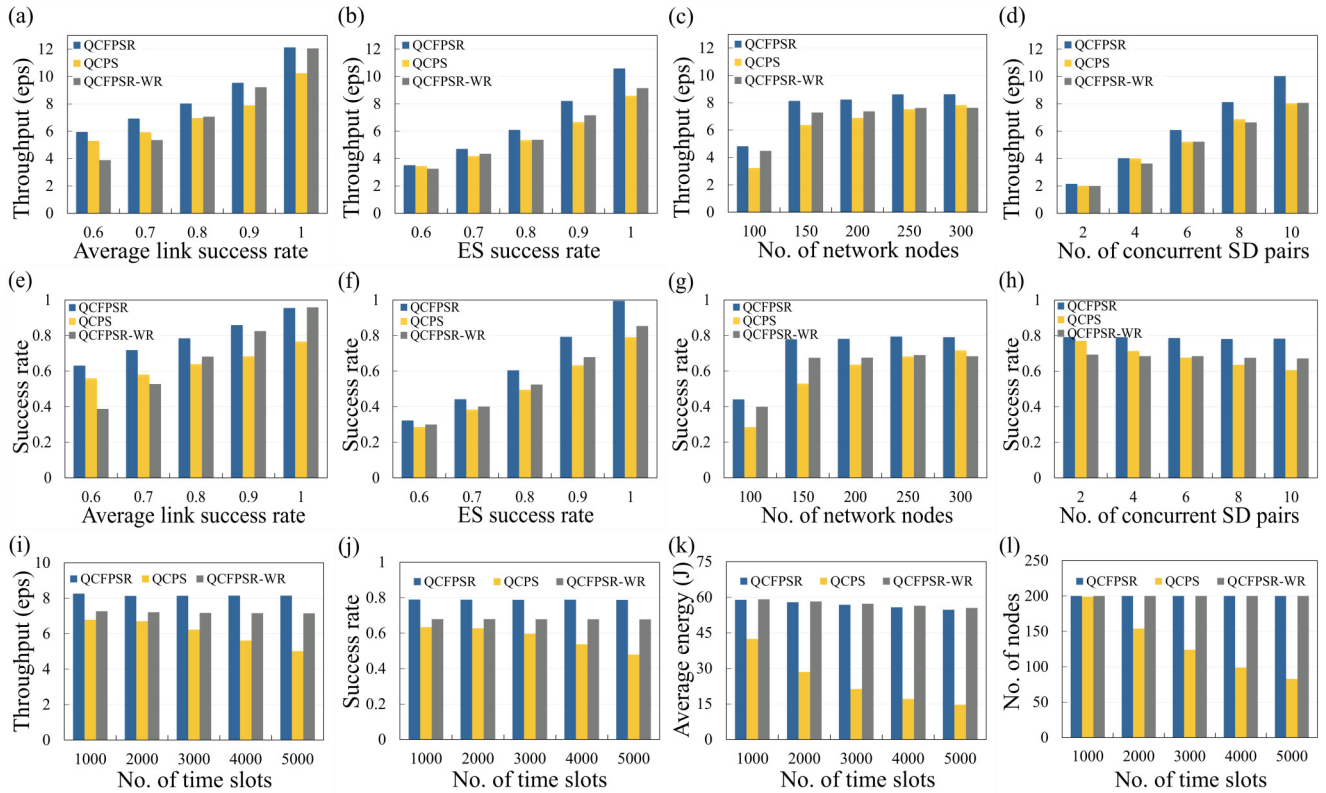


FIG. 8. Performance comparison of QCFPSR, QCPS, and QCFPSR-WR protocols. The throughput (eps denotes the number of entangled qubits per one time slot) is plotted vs (a) the average link success rate, (b) the ES success rate, (c) the number of network nodes, and (d) the number of concurrent SD pairs. The success rate is plotted vs (e) the average link success rate, (f) the ES success rate, (g) the number of network nodes, and (h) the number of concurrent SD pairs. The (i) throughput, (j) success rate, (k) average energy, and (l) number of nodes are plotted vs the number of time slots.

In the following we will evaluate the performance of the QCPS, QCFPSR, and QCFPSR-WR protocols in terms of throughput and success rate by simulations and verify the effectiveness of the proposed routing protocol. Meanwhile, simulations can provide suitable parameters for the real scenes as a reference.

D. Simulation results

We apply various combinations of parameters and analyze the impact of these parameters on the performance of the protocols. Under the condition of different average link success rates, entanglement swapping rates, number of network nodes, number of concurrent SD pairs, and number of time slots, the variations in throughput, success rates, average energy, and number of nodes of QCFPSR, QCPS, and QCFPSR-WR protocols are shown in Fig. 8.

Figures 8(a) and 8(e) show that the throughput and the success rate increase with average link success rates in QCFPSR, QCPS, and QCFPSR-WR protocols. From these two figures, we can draw the following conclusions. First, due to no path conflict and resource contention in the QCFPSR protocol, the throughput and success rate of the QCFPSR protocol are consistently higher than that of the QCPS protocol. Second, due to the link failures in phase 2, the QCFPSR-WR protocol exhibits lower throughput and success rate than the QCFPSR and QCPS protocols when the average link rate is low. Third,

when the average link success rate exceeds 0.8, the performance of the QCFPSR-WR protocol is similar to that of the QCFPSR protocol and outperforms the QCPS protocol. In this case, the QCFPSR-WR protocol can be used instead of the QCFPSR protocol to improve the efficiency of the protocol.

Figures 8(b) and 8(f) depict the impact of entanglement swapping (ES) success rates on throughput and success rate in the QCFPSR, QCPS, and QCFPSR-WR protocols. We can see from the figures that the entanglement swapping success rate has the greatest impact on throughput and success rate. When the entanglement swapping success rate is low, the throughput and success rate of these protocols are approximately equal. This is because the link failures can be mitigated by the path recovery phase, but the entanglement swapping errors cannot be restrained.

Figures 8(c) and 8(g) show that the throughput and success rate vary with the number of network nodes in the QCFPSR, QCPS, and QCFPSR-WR protocols. For the QCPS protocol, the number of nodes has a great impact on performance. When the nodes in the network are sparse, there are more conflicts and competitions for quantum resources in path selection. For the QCFPSR and QCFPSR-WR protocols, the throughput and success rate increase slightly when the number of network nodes reaches a certain value. Therefore, we may strike a good balance between resources and performance in the network.

Figure 8(d) shows that the throughput increases with the number of concurrent SD pairs, where the QCFPSR protocol

shows great advantages over the QCPS protocol as the number of concurrent nodes increases. Figure 8(h) shows that the success rate decreases as the number of concurrent SD pairs increases, with the QCPS protocol decreasing rapidly. This is because more concurrent SD pairs in one time slot introduce a higher level of resource conflicts.

Figures 8(i)–8(l) exhibit the throughput, success rate, average energy, and number of nodes varying with the number of time slots in the reference setting in the QCFPSR, QCPS, and QCFPSR-WR protocols. When the number of time slots exceeds 1000, the nodes in the QCPS protocol gradually drop out of the network due to insufficient residual energy. When the number of time slots reaches 5000, the average residual energy in the QCPS protocol is 25% of the node initial energy and 60% of the nodes are inactive, while the average residual energy in the QCFPSR and QCFPSR-WR protocols is still 90% of the initial energy and almost all nodes are active. As the number of time slots increases, the throughput and success rate of the QCPS protocol decrease rapidly, while both the throughput and success rate of the QCFPSR and QCFPSR-WR protocols remain stable. Therefore, the QCFPSR and QCFPSR-WR protocols significantly outperform the QCPS protocol in terms of network lifetime.

Summary of evaluations. The QCFPSR protocol exhibits much higher throughput and success rate and longer network lifetime than the QCPS protocol. If the average link success rate exceeds a certain value, the recovery path discovery phase can be disabled for better efficiency. The QCFPSR-WR protocol strikes a good balance between performance and efficiency.

VI. CONCLUSION AND FUTURE WORK

This work has presented a comprehensive entanglement routing protocol for QWNs, which can construct contention-free paths for concurrent communication. Simulation results showed that the proposed protocol outperforms existing quantum wireless network routing protocols in terms of throughput, success rate, and network lifetime. We expect that our study can serve as a basis for future exploration of entanglement routing in QWNs.

There is much potential for related future work on the topic of routing protocols in QWNs. Three possible research topics related to this work are designing a more fair protocol for concurrent communication requests, exploration of the optimal recovery paths when nodes share link states with k -hop neighbors, and the reasonable deployment of nodes to achieve efficient communication.

ACKNOWLEDGMENTS

This research was financially supported by the National Key Research and Development Program of China (Grant No. 2017YFA0303704), the Major Program of National Natural Science Foundation of China (Grants No. 11690030 and No. 11690032), the National Natural Science Foundation of China (Grant No. 61771236), the Natural Science Foundation of Jiangsu Province (Grant No. BK20190297), Nanjing University Innovation Program for Ph.D. candidates, and Collaborative Innovation Center of Novel Software Technology and Industrialization.

-
- [1] M. Gong, S. Wang, C. Zha, M.-C. Chen, H.-L. Huang, Y. Wu, Q. Zhu, Y. Zhao, S. Li, S. Guo *et al.*, Quantum walks on a programmable two-dimensional 62-qubit superconducting processor, *Science* **372**, 948 (2021).
 - [2] R. Blatt and C. F. Roos, Quantum simulations with trapped ions, *Nat. Phys.* **8**, 277 (2012).
 - [3] M.-R. Yun, F.-Q. Guo, L.-L. Yan, E. Liang, Y. Zhang, S.-L. Su, C. X. Shan, and Y. Jia, Parallel-path implementation of nonadiabatic geometric quantum gates in a decoherence-free subspace with nitrogen-vacancy centers, *Phys. Rev. A* **105**, 012611 (2022).
 - [4] L. Sansoni, F. Sciarrino, G. Vallone, P. Mataloni, A. Crespi, R. Ramponi, and R. Osellame, Two-Particle Bosonic-Fermionic Quantum Walk via Integrated Photonics, *Phys. Rev. Lett.* **108**, 010502 (2012).
 - [5] P. Busch, T. Heinonen, and P. Lahti, Heisenberg’s uncertainty principle, *Phys. Rep.* **452**, 155 (2007).
 - [6] W. K. Wootters and W. H. Zurek, A single quantum cannot be cloned, *Nature (London)* **299**, 802 (1982).
 - [7] C. H. Bennett and G. Brassard, Quantum cryptography: Public key distribution and coin tossing, *Theor. Comput. Sci.* **560**, 7 (2014).
 - [8] A. K. Ekert, Quantum Cryptography Based on Bell’s Theorem, *Phys. Rev. Lett.* **67**, 661 (1991).
 - [9] M. Żukowski, A. Zeilinger, M. A. Horne, and A. K. Ekert, “Event-ready-detectors” Bell Experiment via Entanglement Swapping, *Phys. Rev. Lett.* **71**, 4287 (1993).
 - [10] C. Elliott, Building the quantum network, *New J. Phys.* **4**, 46 (2002).
 - [11] J.-W. Pan, D. Bouwmeester, H. Weinfurter, and A. Zeilinger, Experimental Entanglement Swapping: Entangling Photons That Never Interacted, *Phys. Rev. Lett.* **80**, 3891 (1998).
 - [12] M. Peev, C. Pacher, R. Alléaume, C. Barreiro, J. Bouda, W. Boxleitner, T. Debuisschert, E. Diamanti, M. Dianati, J. Dynes *et al.*, The SECOQC quantum key distribution network in Vienna, *New J. Phys.* **11**, 075001 (2009).
 - [13] M. Sasaki, M. Fujiwara, H. Ishizuka, W. Klaus, K. Wakui, M. Takeoka, S. Miki, T. Yamashita, Z. Wang, A. Tanaka *et al.*, Field test of quantum key distribution in the tokyo QKD network, *Opt. Express* **19**, 10387 (2011).
 - [14] J. Yin, Y. Cao, Y.-H. Li, S.-K. Liao, L. Zhang, J.-G. Ren, W.-Q. Cai, W.-Y. Liu, B. Li, H. Dai *et al.*, Satellite-based entanglement distribution over 1200 kilometers, *Science* **356**, 1140 (2017).
 - [15] T. Inagaki, N. Matsuda, O. Tadanaga, M. Asobe, and H. Takesue, Entanglement distribution over 300 km of fiber, *Opt. Express* **21**, 23241 (2013).
 - [16] H.-L. Yin, T.-Y. Chen, Z.-W. Yu, H. Liu, L.-X. You, Y.-H. Zhou, S.-J. Chen, Y. Mao, M.-Q. Huang, W.-J. Zhang, H. Chen, M. J. Li, D. Nolan, F. Zhou, X. Jiang, Z. Wang, Q. Zhang, X.-B. Wang, and J.-W. Pan, Measurement-Device-Independent Quantum Key Distribution Over a 404 km Optical Fiber, *Phys. Rev. Lett.* **117**, 190501 (2016).
 - [17] J. Qiu, Quantum communications leap out of the lab, *Nature (London)* **508**, 441 (2014).

- [18] H.-Y. Liu, X.-H. Tian, C. Gu, P. Fan, X. Ni, R. Yang, J.-N. Zhang, M. Hu, J. Guo, X. Cao *et al.*, Drone-based entanglement distribution towards mobile quantum networks, *Natl. Sci. Rev.* **7**, 921 (2020).
- [19] E. Semsch, M. Jakob, D. Pavlicek, and M. Pechoucek, in *Proceedings of the IEEE/WIC/ACM International Conference on Web Intelligence and Intelligent Agent Technology Workshops, Milan, 2009*, edited by P. Boldi, G. Vizzari, G. Pasi, and R. Baeza-Yates (IEEE, Piscataway, 2009), Vol. 2, pp. 82–85.
- [20] J. G. Manathara, P. Sujit, and R. W. Beard, Multiple UAV coalitions for a search and prosecute mission, *J. Intell. Robot Syst.* **62**, 125 (2011).
- [21] I. Maza, F. Caballero, J. Capitán, J. R. Martínez-de Dios, and A. Ollero, Experimental results in multi-UAV coordination for disaster management and civil security applications, *J. Intell. Robot Syst.* **61**, 563 (2011).
- [22] A. Cho, J. Kim, S. Lee, and C. Kee, Wind estimation and airspeed calibration using a UAV with a single-antenna GPS receiver and pitot tube, *IEEE Trans. Aerosp. Electron. Syst.* **47**, 109 (2011).
- [23] K.-S. Chung and J.-E. Lee, Design and development of machine learning service based on 3G cellular phones, *J. Inf. Process. Syst.* **8**, 521 (2012).
- [24] H. Luo and M.-L. Shyu, Quality of service provision in mobile multimedia—A survey, *Hum. Cent. Comput. Inf. Sci.* **1**, 5 (2011).
- [25] G. Marques, R. Pitarma, N. M. Garcia, and N. Pombo, Internet of things architectures, technologies, applications, challenges, and future directions for enhanced living environments and healthcare systems: A review, *Electronics* **8**, 1081 (2019).
- [26] C. Barrado, R. Messeguer, J. López, E. Pastor, E. Santamaria, and P. Royo, Wildfire monitoring using a mixed air-ground mobile network, *IEEE Pervas. Comput.* **9**, 24 (2010).
- [27] E. P. De Freitas, T. Heimfarth, I. F. Netto, C. E. Lino, C. E. Pereira, A. M. Ferreira, F. R. Wagner, and T. Larsson, in *Proceedings of the International Congress on Ultra Modern Telecommunications and Control Systems, Moscow, 2010* (IEEE, Piscataway, 2010), pp. 309–314.
- [28] S.-T. Cheng, C.-Y. Wang, and M.-H. Tao, Quantum communication for wireless wide-area networks, *IEEE J. Sel. Area. Commun.* **23**, 1424 (2005).
- [29] Z.-Z. Li, G. Xu, X.-B. Chen, X. Sun, and Y.-X. Yang, Multi-user quantum wireless network communication based on multi-qubit GHZ state, *IEEE Commun. Lett.* **20**, 2470 (2016).
- [30] H. Qi, T. Xiao, and Y. Guo, in *Proceedings of the 15th IEEE International Symposium on Parallel and Distributed Processing with Applications and 16th IEEE International Conference on Ubiquitous Computing and Communications, Guangzhou, 2017*, edited by G. Wang, G. Fox, G. Martinez, R. Hill, and P. Mueller (IEEE, Piscataway, 2017), pp. 1422–1426.
- [31] K. Wang, X. T. Yu, S. L. Lu, and Y. X. Gong, Quantum wireless multihop communication based on arbitrary bell pairs and teleportation, *Phys. Rev. A* **89**, 022329 (2014).
- [32] K. Wang, Y.-X. Gong, X.-T. Yu, and S.-L. Lu, Addendum to “Quantum wireless multihop communication based on arbitrary Bell pairs and teleportation”, *Phys. Rev. A* **90**, 044302 (2014).
- [33] X.-Q. Gao, Z.-C. Zhang, and B. Sheng, Multi-hop teleportation in a quantum network based on mesh topology, *Front. Phys.* **13**, 130314 (2018).
- [34] R. Cai, X.-T. Yu, and Z.-C. Zhang, Bidirectional teleportation protocol in quantum wireless multi-hop network, *Int. J. Theor. Phys.* **57**, 1723 (2018).
- [35] Y.-G. Yang, S.-N. Cao, Y.-H. Zhou, and W.-M. Shi, Quantum wireless network communication based on cluster states, *Mod. Phys. Lett. A* **35**, 2050178 (2020).
- [36] P.-Y. Xiong, X.-T. Yu, Z.-C. Zhang, H.-T. Zhan, and J.-Y. Hua, Routing protocol for wireless quantum multi-hop mesh backbone network based on partially entangled GHZ state, *Front. Phys.* **12**, 120302 (2017).
- [37] X.-T. Yu, X. Jin, and Z.-C. Zhang, Distributed wireless quantum communication networks, *Chinese Phys. B* **22**, 090311 (2013).
- [38] W. C. Huang, Source code for quantum wireless networks entanglement routing simulations, <https://github.com/WeicongHuang/QWN-Routing> (2022).
- [39] D. B. Johnson and D. A. Maltz, in *Mobile Computing*, edited by T. Imielinski and H. F. Korth, The Kluwer International Series in Engineering and Computer Science Vol. 353 (Springer, Boston, 1996), pp. 153–181.
- [40] C. E. Perkins and E. M. Royer, in *Proceedings of the Second IEEE Workshop on Mobile Computing Systems and Applications, New Orleans, 1999* (IEEE, Piscataway, 1999), pp. 90–100.
- [41] M. Caleffi, Optimal routing for quantum networks, *IEEE Access* **5**, 22299 (2017).
- [42] A. Dahlberg, M. Skrzypczyk, T. Coopmans, L. Wubben, F. Rozpedek, M. Pompili, A. Stolk, P. Pawelczak, R. Knegiens, J. de Oliveira Filho *et al.*, in *Proceedings of the ACM Special Interest Group on Data Communication, Beijing, 2019* (ACM, New York, 2019), pp. 159–173.
- [43] M. Pant, H. Krovi, D. Towsley, L. Tassiulas, L. Jiang, P. Basu, D. Englund, and S. Guha, Routing entanglement in the quantum internet, *npj Quantum Inf.* **5**, 25 (2019).
- [44] S. Shi and C. Qian, in *Proceedings of the Annual Conference of the ACM Special Interest Group on Data Communication on the Applications, Technologies, Architectures, and Protocols for Computer Communication* (ACM, New York, 2020), pp. 62–75.
- [45] J. Aspnes, Y. Azar, A. Fiat, S. Plotkin, and O. Waarts, in *Proceedings of the 25th Annual ACM Symposium on Theory of Computing, San Diego, 1993* (ACM, New York, 1993), pp. 623–631.
- [46] B. Awerbuch, R. Gawlick, T. Leighton, and Y. Rabani, in *Proceedings 35th Annual Symposium on Foundations of Computer Science, Santa Fe, 1994* (IEEE, Piscataway, 1994), pp. 412–423.
- [47] F. P. Kelly, Routing in circuit-switched networks: Optimization, shadow prices and decentralization, *Adv. Appl. Probab.* **20**, 112 (1988).
- [48] R. Horodecki, P. Horodecki, M. Horodecki, and K. Horodecki, Quantum entanglement, *Rev. Modern Phys.* **81**, 865 (2009).
- [49] P. C. Humphreys, N. Kalb, J. P. Morits, R. N. Schouten, R. F. Vermeulen, D. J. Twitchen, M. Markham, and R. Hanson, Deterministic delivery of remote entanglement on a quantum network, *Nature (London)* **558**, 268 (2018).
- [50] H. J. Briegel, W. Dür, J. I. Cirac, and P. Zoller, Quantum Repeaters: The Role of Imperfect Local Operations in Quantum Communication, *Phys. Rev. Lett.* **81**, 5932 (1998).
- [51] N. Sangouard, C. Simon, H. de Riedmatten, and N. Gisin, Quantum repeaters based on atomic ensembles and linear optics, *Rev. Mod. Phys.* **83**, 33 (2011).

- [52] A. Carrasco-Casado, V. Fernández, and N. Denisenko, in *Optical Wireless Communications*, edited by M. Uysal, C. Capsoni, Z. Ghassemlooy, A. Boucouvalas, and E. Udvary (Springer, Cham, 2016), pp. 589–607.
- [53] J. Yan, M. Zhou, and Z. Ding, Recent advances in energy-efficient routing protocols for wireless sensor networks: A review, *IEEE Access* **4**, 5673 (2016).
- [54] P. Komar, E. M. Kessler, M. Bishof, L. Jiang, A. S. Sørensen, J. Ye, and M. D. Lukin, A quantum network of clocks, *Nat. Phys.* **10**, 582 (2014).
- [55] E. Ziouva and T. Antonakopoulos, CSMA/CA performance under high traffic conditions: Throughput and delay analysis, *Comput. Commun.* **25**, 313 (2002).
- [56] Y. Xu, J. Heidemann, and D. Estrin, in *Proceedings of the Seventh Annual International Conference on Mobile Computing and Networking, Rome, 2001* (ACM, New York, 2001), pp. 70–84.
- [57] X. Cheng, A. Thaeler, G. Xue, and D. Chen, in *Proceedings of the 23rd Annual Joint Conference of the IEEE Computer and Communications Societies, Hong Kong, 2004* (IEEE, Piscataway, 2004), Vol. 4, pp. 2685–2696.
- [58] A. Thaeler, M. Ding, and X. Cheng, iTPS: An improved location discovery scheme for sensor networks with long-range beacons, *J. Parallel Distr. Comput.* **65**, 98 (2005).
- [59] Y. Xue, B. Li, and K. Nahrstedt, in *Proceedings of the 26th Annual IEEE Conference on Local Computer Networks, Tampa, 2001* (IEEE, Piscataway, 2001), pp. 102–111.